

# Propagation of intense short-pulse laser in homogeneous near-critical density plasmas

H Habara<sup>1</sup>, S Nakaguchi<sup>1</sup>, Y Uematsu<sup>1</sup>, S D Baton<sup>2</sup>, S N Chen<sup>2</sup>, J Fuchs<sup>2</sup>,  
T Iwawaki<sup>1</sup>, M MacDonald<sup>3,4</sup>, W Nazarov<sup>5</sup>, C Rousseaux<sup>6</sup> and K A Tanaka<sup>1</sup>

<sup>1</sup>Osaka University, Suita, Osaka, Japan

<sup>2</sup>LULI, Ecole Polytechnique, Palaiseau, France

<sup>3</sup>University of Michigan, Ann Arbor, MI, USA

<sup>4</sup>SLAC National Accelerator Laboratory, Menlo Park, CA, USA

<sup>5</sup>University of St. Andrews, St. Andrews, Scotland, United Kingdom

<sup>6</sup>CEA, DAM, DIF, Arpajon, France

habara@eei.eng.osaka-u.ac.jp

**Abstract.** Ultra intense laser light propagation in a homogeneous overdense plasma was investigated using a plastic foam target filling a polyimide tube. Laser propagation into overdense plasma was measured via Doppler red shift of the reflected laser light from the moving plasma at 0.3-0.4 of speed of light. We also observed strongly collimated electron beam possibly caused by the magnetic field surrounding the plasma channel, and high energy X-rays emitted via synchrotron radiation by the oscillating electrons inside the channel. These features imply that UIL propagates inside the overdense plasma as predicted in PIC calculation, and are very important for direct irradiation scheme of fast ignition.

## 1. Introduction

Ultra intense laser (UIL) light can propagate in overdense plasma due to relativistic effects. For example, relativistic transparency enables the UIL propagation by effective reduction of the electron plasma frequency through the apparent electron mass enhancement. Increase of laser intensity by relativistic self-focusing of Gaussian beam also reinforces the transparency effect. We adapted these effects into Fast Ignition in order to make UIL accessible to the core plasma as close as possible [1]. For several years, we have investigated the UIL propagation into an implosion or a blow-off plasma having not only overdense but also long underdense regions. However, the investigation using these plasmas was somehow difficult because the critical density ( $N_c$ ) position and/or the density scale length are not clear in such plasma. In addition, because UIL becomes unstable before reaching  $N_c$  by suffering several laser-plasma instabilities such as filamentation or bifurcation [2], quantitative discussions regarding the overdense region are difficult for reproducibility issues.

In order to overcome these difficulties, we performed an experiment to create characterized homogeneous plasmas (electron density of 0.8 and 1.3 $N_c$ ) over 300 $\mu$ m at ELFIE facility in LULI, Ecole Polytechnique, France [3]. In this experiment, we observed a significantly collimated electron beam ( $\sim 11^\circ$  FWHM) along the laser direction, possibly caused by magnetic collimation along the plasma channel. This result strongly suggests laser propagation into the overdense plasma [4]. In order to confirm these results, we recently performed an experiment for UIL propagation in this plasma



where Doppler reflectometry of the backscattered light was measured in order to understand the propagation speed in the plasma.

## 2. Experimental setup

Figure 1 shows the experimental setup. In order to create a homogeneous plasma, a low-density plastic ( $C_{15}H_{20}O_6$ ) foam target ( $\rho \sim 5$  and  $10 \text{ mg/cc}$ ) was inserted in a polyimide tube having  $300 \mu\text{m}$  diameter and  $300 \mu\text{m}$  length. A thin Cu foil ( $700 \text{ nm}$ ,  $5 \times 5 \text{ mm}^2$ ) was attached at the one side of the tube entrance hole. A sub-ns chirped pulse irradiated this foil with  $500 \mu\text{m}$  spot diameter to create X-rays which ionized the foam uniformly. Finally, an ultra intense laser light ( $1\omega (=1054 \text{ nm})$ ,  $10 \text{ J}/300 \text{ fs}$  -  $3 \times 10^{19} \text{ W/cm}^2$ ) was focused into the foam plasma from the opposite entrance hole. The backscattered light was collected using a beam splitter located before the focusing off-axis parabola, and was then split to a photodiode and a spectrometer outside the interaction chamber. The electron energy spectra and electron emission distribution were observed in the laser propagation direction. Angular distribution of X-ray intensity was also obtained with the help of an imaging plate.

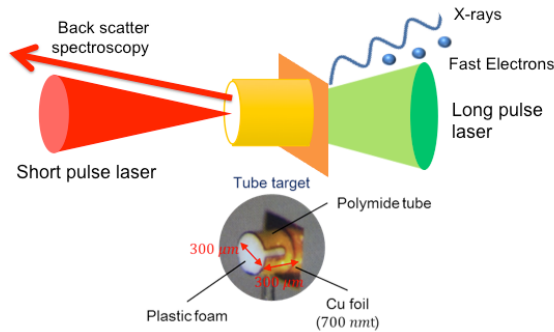


Fig.1 Experimental setup.

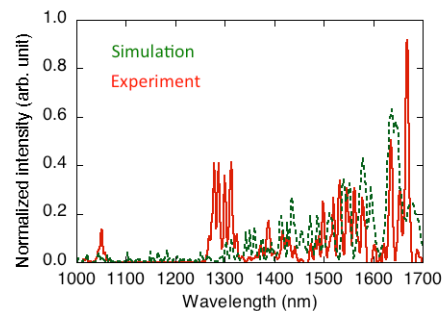


Fig.2 Backscattered light spectra from experiment (dashed line) and simulation (solid line).

## 3. Doppler reflectometry

Reflected spectra show a significant red shift for both foam densities. The solid curve in Fig. 2 indicates a typical experimental spectrum from  $5 \text{ mg/cc}$  foam plasma irradiated by UIL. Typically, the peak of the reflected light appeared at  $0.6\omega$  ( $1.7 \mu\text{m}$ ) for  $5 \text{ mg/cc}$  foam and  $0.7\omega$  ( $1.55 \mu\text{m}$ ) for  $10 \text{ mg/cc}$  foam target, respectively. Here, the reflected light energies were about 5.3% and 7.2% of the incident laser energy for 5 and  $10 \text{ mg/cc}$  plasmas respectively. These values are somehow similar to the observation in the relativistic laser region [5,6]. However, our plasma density is much higher than those experiments and is not favorable for Raman development even in relativistic regime. In addition, we only had a very short underdense plasma (could be less than a few microns) whereas SRS is very sensitive to the laser propagation length. In fact, we observed very similar reflected laser energies when the pulse width was stretched to  $900 \text{ fs}$  and  $1.5 \text{ ps}$ , whereas longer laser pulses were expected to drive more SRS in underdense plasma [5]. From these considerations we believe that the red shift was caused by Doppler shift at the moving piled up plasma at the laser front, rather than SRS. In this model, the plasma electrons inside the laser volume oscillate in the laser field at relativistic energies, with the result that the Lorentz factor of these electrons becomes larger than those at outside the laser region [7-9]. The local enhancement of the Lorentz factor results in a significant gap of the plasma frequency at the laser front, which acts as a mirror for the laser light. This surface moves with a velocity determined by the energy balance between the radiation pressure and the kinetic pressure around the surface, which is much slower than the relativistic group velocity given at its density.

Adapting this model, the experimental Doppler shifts ( $0.6\omega$  and  $0.7\omega$ ) give the mirror speed of  $0.46c$  and  $0.36c$  for 5 and  $10 \text{ mg/cc}$  foams respectively. We also calculated the analytical recession velocity of the piled up plasma for various laser intensities and plasma density conditions, which shows that the experimental mirror speeds correspond to  $1N_c$  and  $2N_c$  plasmas with  $2\text{--}3 \times 10^{19} \text{ W/cm}^2$  [8,9] in 5 and  $10 \text{ mg/cc}$  foams, in agreement with the experimental laser and plasma conditions. This

model was evaluated with 1D and 2D PIC calculations [8,9]. The simulated reflected light spectrum for  $1N_c$  plasma with  $I_L=3\times10^{19}\text{W/cm}^2$ , as shown in dashed curve in Fig.2, also well reproduced the experimental one.

#### 4. Electron measurement

We also observed the electron emission distribution by using a large image plate at the back side of the target with respect to the UIL direction. Figure 3 indicates the emission pattern obtained for (a) 5mg/cc foam target and (b) Al 50 $\mu\text{m}$  foil target. In order to assess the signal produced by electrons only, PET (Polyethylene terephthalate) plate 1mm and Al 12 $\mu\text{m}$  filters were inserted in front of imaging plate. These filters reject less than 1-keV X-rays and several MeV protons, so that the IP only records electrons having over 100-keV kinetic energies. Note that the detection probability of the image plate over 100-keV electrons is almost constant [9]. The horizontal black line in the middle of Fig. 3(a) represents the slit of the multi-channel electron spectrometer.

As shown in Fig.3, the electron emission pattern of the foam target (Fig. 3a) exhibits a significant reduction of beam divergence ( $10^\circ$ - $20^\circ$  in FWHM), compared to that obtained from the aluminum foil ( $> 40^\circ$ ) (Fig. 3(b)), as observed in a previous paper [4]. With foam targets, the multi-channel spectrometer ESM ( $0^\circ$ - $20^\circ$ ) also shows the increase of the electron number observed near the peak position of the emission signal, compared to the side position, whereas no difference was observed with foil targets (not presented here).

2D PIC calculations also reproduce the beam collimation in the homogeneous plasma as already shown in a previous paper [8]. The calculation also indicates that the UIL creates a plasma channel inside the overdense plasma and a strong magnetic field along the plasma channel. This strong magnetic field collimates the fast electrons toward the laser direction. In order to check this collimation, we calculated trajectories of electrons having an initially isotropic emission distribution at the entrance of the field. We observed that the lower energy electrons are trapped inside the magnetic field, whereas the higher energy electrons are delivered toward the laser propagation direction, resulting in the collimation of the electron beam. The result of electron measurements also indicates laser propagation inside  $N_c$  plasma.

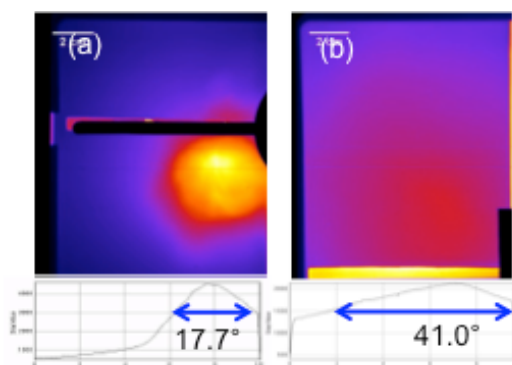


Fig.3 Emission distribution of fast electrons from (a) foam target and (b) Al 50 $\mu\text{m}$  foil target.

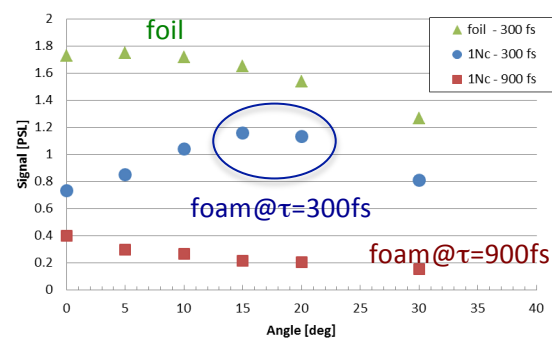


Fig.4 Angular distributions of X-ray emission for various conditions; Foam 5mg/cc,  $I=3\times10^{19}\text{W/cm}^2$  (circles),  $I=1\times10^{19}\text{W/cm}^2$  (squares), Al foil,  $I=3\times10^{19}\text{W/cm}^2$  (triangles).

#### 5. X-ray measurement

Angular distribution of X-ray intensity was separately measured from the electron measurement. An array of image plates was set in the laser direction from 0 to 30 degrees, every  $5^\circ$ , each one having an aperture of 4 msr. The electrons were removed from the path to the image plate by using strong magnets. We also inserted the PET and the Al filters, in order to record only X-rays over 1-keV. Figure 4 represents the angular distribution of X-rays for different conditions: foam 5mg/cc,  $I=3\times10^{19}\text{W/cm}^2$  /  $\tau=300\text{fs}$  (circles) and  $I=1\times10^{19}\text{W/cm}^2$  /  $\tau=900\text{fs}$  (squares), Al foil,  $I=3\times10^{19}\text{W/cm}^2$  /

$\tau=300\text{fs}$  (triangles). A side peak (at  $15^\circ\text{-}20^\circ$  from the laser direction) is only observed with the foam plasma in the highest intensity case. If the X-rays were created via Bremsstrahlung emission, they should have a peak emission corresponding to the electron emission direction ( $0^\circ\text{-}10^\circ$ ) [11], which is observed in the cases of Al foil and lower intensity foam targets. On the other hand, for synchrotron radiation, the X-ray peak emission is expected around  $\theta\sim 16^\circ$  for our experimental conditions (laser intensity and plasma density) [12], which well agrees with the observation.

In order to better characterize the radiation mechanism of the side peak emission, we additionally inserted a 1 mm Cu filter in front of the image plate. Thus, the intensity around the side peak emission was reduced to 13% of the one without Cu filter. From this attenuation rate, the X-ray energy is estimated around 53keV. Analytically, the X-ray energy of synchrotron radiation given our experimental conditions is calculated to be 51.2keV [11], which well agrees with the experimental value. In addition, assuming that most of the X-rays are created through synchrotron radiation in a symmetry perpendicular to the polarization plane, the total X-ray photon number and energy are estimated to  $5\times 10^{10}$  and 0.4mJ, respectively. According to Ref. [13],  $7\times 10^{12}$  electrons are required to generate these photons; therefore the total energy of electrons is about 10% of the laser energy. From these estimations, we believe that the synchrotron radiation predominates the X-ray emission in the foam target case at the highest laser intensity. The observation of synchrotron radiation suggests electron oscillation inside the plasma channel, and therefore that the laser propagates in the dense plasma.

## 6. Summary

We have investigated ultra intense laser light propagation in a long, homogeneous, overdense plasma using a plastic foam target filling a polyimide tube. Laser propagation into overdense plasma was investigated via Doppler red shift of the reflected laser light from the moving plasma at 0.3-0.4 speed of light. The observed electron beam was strongly collimated probably by the magnetic field surrounding the plasma channel. High energy X-rays were emitted via synchrotron radiation by the oscillated electrons inside the channel. These features imply that UIL propagates inside the overdense plasma as predicted by PIC calculations. These results are very important for direct irradiation scheme of fast ignition.

## Acknowledgement

The authors gratefully acknowledge the support of the staff of the ELFIE in the execution of this work (14TWF1). We also thank Professor H. Sakagami at National Institute for Fusion Science for his permission of use of 2D-PIC FISCOF code. A part of this work is supported by Grants-in-Aid for Scientific Research, type S (Grant No. 15H05751).

## References

- [1] A.L. Lei *et al.*, Phys. Plasmas **16** (2009) 056307.
- [2] G. Li *et al.*, Phys. Rev. Lett. **100** (2008) 125002.
- [3] S.N. Chen *et al.*, Sci. Report **6** (2016) 21495.
- [4] T. Iwawaki *et al.*, Phys. Plasmas **21** (2014) 113103.
- [5] C. Rousseaux *et al.*, Phys. Plasmas. **9** (2002) 4261.
- [6] T. Miyakoshi *et al.*, Phys. Plasmas **9** (2002) 3552.
- [7] S. Guerin, P. Mora, J. C. Adam, A. H'eron, and G. Laval, Phys. Plasmas **3** (1996) 2693.
- [8] T. Iwawaki *et al.*, Phys. Rev. E **92** (2015) 013106.
- [9] T. Iwawaki, Osaka Unverisity, 2015, Ph.D. thesis (in Japanese).
- [10] K.A. Tanaka *et al.*, Rev. Sci. Instrum. **76** (2005) 013507.
- [11] J. D. Jackson, *Classical Electrodynamics* (Wiley, New York, 1975).
- [12] K.T. Phuoc *et al.*, Phys. Plasmas **12** (2005) 023101.
- [13] I. Kostyukov *et al.*, Phys. Plasmas **10** (2003) 4818.